Published on 29 July 2016. Downloaded by Beijing Institute of Nanoenergy and Nanosystems CAS on 16/08/2016 02:10:30.

Journal of Materials Chemistry C

PAPER

View Article Online
View Journal

Cite this: DOI: 10.1039/c6tc02610a

Rational design of an ITO/CuS nanosheet network composite film as a counter electrode for flexible dye sensitized solar cells

Xiaojia Zhang,† Xingqiang Liu,† Yupeng Zhang, Rongrong Bao, Dengfeng Peng, Tianfeng Li, Guoyun Gao, Wenxi Guo and Caofeng Pan*

Received 24th June 2016,
Accepted 28th July 2016

DOI: 10.1039/c6tc02610a

www.rsc.org/MaterialsC

The brittleness of traditional indium-doped tin oxide (ITO) is an obstacle to its commercialization in flexible opto-electronics. Here, we report a flexible ITO/CuS nanosheet network (NN) composite conductive film, with appreciable transparency, by employing a combined electrospinning and sputtering method. 6% power conversion efficiency (PCE) was achieved from the fabricated high-performance flexible dye-sensitized solar cell, in which the ITO/CuS NN composite film serves as the counter electrode and titanium dioxide nanotube arrays (TNARs) as the photoanode. After 200 bending cycles, the PCE presents negligible changes in PCE. The composite films exhibit robust flexibility and electrochemical catalytic properties by taking advantage of CuS NN. We believed that the rationally designed ITO/CuS NN composite transparent conductive electrode can be a promising candidate in portable and wearable electronics.

Introduction

Dye-sensitized solar cells (DSSCs), as one of the promising renewable energy resources, have received great attention in recent years due to their low cost and light weight and the availability of continuous roll-to-roll fabrication methods.[1–5] Indium tin oxide (ITO) is widely used as a conductive layer in DSSCs to achieve transparency and conductivity simultaneously.[3,6–8] However, the poor electrochemical catalytic properties, coupled with inferior chemical stability, rules out the possibility that ITO can be directly used as counter electrodes (CEs) in DSSCs.[9,10] Traditionally, platinum particles overlay the surface of ITO electrodes to cope with the aforementioned obstacle, however this pushes up the cost of the whole fabrication.[11–13] Several Pt-free CEs, such as graphite, carbon black, carbon nanotubes, conducting polymers and CoS, have been explored for flexible DSSCs, and their transparency still needs to be improved, which matters most in the efficiency of DSSCs.[11,14–26] Additionally, instinctively brittle characteristics, easily forming cracks during mechanical deformation, hamper its application in the flexible DSSCs. Alternatives have been reported, for example graphene, carbon nanotubes, conducting polymers, or metal nanowires/nanotroughs.[27–34] Among these potential materials, metal nanotroughs have good transparency, high conductivity and desirable mechanical stability, whereas the poor conductance of non-uniform pitches and high contact resistance caused by large open spaces (>50 μm) are still urgent problems.[35–37] Therefore, it is important to develop a strategy to find a new electrode to fulfil all the demands of CEs in the flexible DSSCs.

Herein, we report a flexible transparent conductive composite ITO/CuS nanosheet network (NN) film, with robust mechanical stability and superior electrochemical catalytic properties, that achieves a relatively low resistance. Flexible DSSCs were fabricated with the ITO/CuS NN composite films as CEs and titanium dioxide nanotube arrays (TNARs) as photoanodes, and obtained a power conversion efficiency (PCE) of 6%, a short current density (J_{sc}) of 18.8 mA cm^{-2} and an open voltage (V_{oc}) of 0.681 V. After 200 cycles of folding and unfolding, the PCE of the as-fabricated flexible solar cell presents negligible change, demonstrating enormous improvement over the intrinsic ITO thin film. The composite films have demonstrated the advantages of the transparency of ITO with the flexibility and superior electrochemical catalytic properties of the CuS NN. This approach thus opens an avenue to flexible transparent conductive electrodes and could not only impact the existing applications, but also expand the novel flexible, transparent and conductive materials which are promising for the opto-electronics area of flexible, wearable, or disposable electronics for computing, storage, and wireless communication.

Experimental

Materials

Sulphur, ethanol, polyvinyl alcohol, NH_4F, $TiCl_4$, ethylene glycol, acetonitrile and methanol were obtained from Sinopharm

Beijing Institute of Nanoenergy and Nanosystems, Chinese Academy of Science, Beijing, China. E-mail: cfpan@binn.cas.cn
† Authors contributed equally to this work.

Published on 29 July 2016. Downloaded by Beijing Institute of Nanoenergy and Nanosystems CAS on 16/08/2016 02:10:30.

Chemical Reagent Co. Ltd, which were analytically pure. N719 dye was obtained from Solaronix. 4-*tert*Butylpyridine, LiI, I_2, and Ti foil were acquired from Sigma-Aldrich.

ITO/CuS NN composite electrode fabrication

Firstly, the PVA fibres were spun on an aluminium frame to form a network and then a Cu film with a thickness of 200 nm was sputtered on the as-prepared PVA fibres. The as-prepared Cu nanofiber networks were transferred onto PET substrates, after removing the PVA fibres in the deionized water. Then the Cu network electrodes were transformed into CuS nanosheet networks by sulphur deposition in a sulphur ethanol solution (0.01 M) at 60 °C for 12 h. The CuS NN electrodes were washed by ethanol after sulphur deposition. Finally, the ITO with a specific thickness of 250 nm was deposited on the as-fabricated CuS nanotrough network by magnetron sputtering at a sputtering power of 100 W (1 h) to prepare the transparent ITO/CuS NN composite electrode at room temperature.

TiO_2 nanotube arrays (TNARs) fabrication

A cleaned Ti foil was immersed into an ethylene glycol solution containing 0.3 wt% NH_4F and 2 vol% H_2O for 9–12 h to finish the anodization process at 50 V using a Pt foil as the counter electrode. Then the as-fabricated titanium dioxide nanotube arrays were peeled off by ultrasonic cleaning for 5 min and dried at 70 °C in an oven in air. Subsequently, the peeled-off Ti foil was anodized in the same ethylene glycol solution for another 3 h to obtain uniformly ordered TNARs. After anodization, the as-prepared titanium nanotube arrays were annealed at 450 °C for 2 h in a muffle roaster in the air. Finally, the highly ordered TNARs were submerged into an aqueous solution containing 0.2 M $TiCl_4$ at 70 °C for 30 minutes followed by annealing at 450 °C for 2 h.

Preparation of DSSCs

The TNARs on Ti foil as photoanodes were submerged into a dye ethanol solution containing 0.5 mM N719 for 24 h, then washed by ethanol and dried at room temperature. The TNAR photoanodes and the ITO/CuS NN composite electrode, the CuS NN electrode or the traditional ITO/PET CEs were installed together using a hot-melt sealed tape (SX1170-25; Solaronix Co.). The electrolyte solution containing 0.5 M LiI, 50×10^{-3} M I_2, and 0.5 M 4-*tert*butylpyridine in 3-methoxypropionitrile (Fluka) was used for the flexible DSSCs.

Characterization

The sheet resistances were measured by a digital multimeter (Keithley 2100) with a four-point probe. The optical transmittance of the ITO/CuS NN composite electrodes and ITO/PET films was measured by UV-vis spectroscopy (Shimadzu UV-3600). The morphology and the EDX of the flexible electrodes were characterized by scanning electron microscopy (SEM, Hitachi SU8020). The XRD spectrum was measured by a PANalytical X'Pert PRO diffractometer. All the cells were tested under a sun simulator (SOLO22A, CROWTECH) at AM 1.5 (100 mW cm^{-2}) by back illumination from the CEs. Electrochemical impedance spectroscopy was measured by an autolab model PGSTAT 30 (ECO-Chemie B.V.) with a Frequency Response Analyzer module (Autolab, Eco-Chemie) and the corresponding frequency ranges from 0.1 Hz to 100 Hz with an amplitude of 10 mV. A Z-view software (Scribner Associates Inc.) was used to process the EIS data. Cyclic voltammograms (CVs) were obtained by using an Autolab electrochemical workstation in the conventional three-electrode system at a scan rate of 50 mV s^{-1} with the voltage range of −0.8 V to 0.8 V. All the measurements were at room temperature in the dark. The devices were bent by a linear motor (Linmot E1100), and the actual bending radius of the loaded devices was measured by fitting circles to images taken by an optical camera mounted facing the edge of the film.

Results and discussion

Fig. 1a presents the schematic images of fabricating the transparent ITO/CuS NN composite film on PET substrates in a combined electrospinning and magnetron sputtering method. First off, PVA fibres were produced by electrospinning with desirable uniformity on the aluminium substrates, followed by Cu sputtering. Then, the as-prepared Cu networks were transferred onto the PET substrate by removing the PVA fibres in deionised water.[35] Then, the Cu NNs were immersed into the ethanol solution containing excess sulphur powder at 60 °C for 12 h. As a result, all the Cu NNs have been transformed into

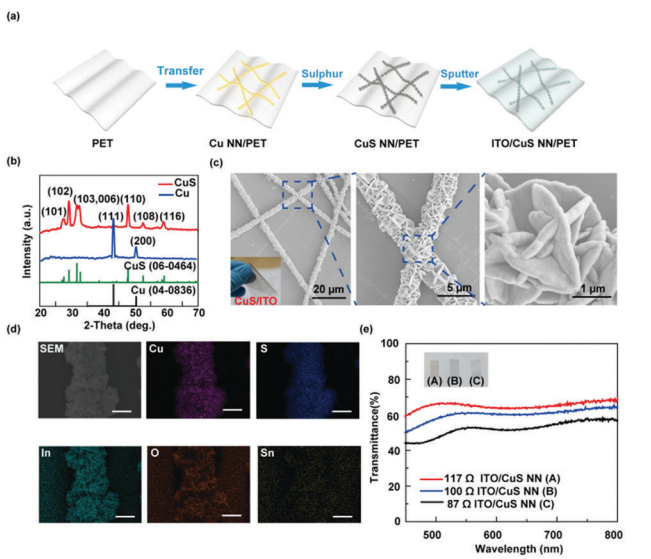

Fig. 1 (a) The schematic image of the fabrication processes of the transparent ITO/CuS NN composite film. (b) XRD patterns of the Cu nanotrough and CuS nanosheet network transparent films, showing the pure phase of the Cu nanotrough and the CuS NN. (c) A photograph and SEM images of the transparent ITO/CuS NN composite film at different magnifications, demonstrating the morphology of the as-prepared ITO/CuS NN. (d) The SEM images and the corresponding energy-dispersive X-ray spectroscopy (EDX) images, presenting the morphology and element distributions in the ITO/CuS NN on the PET substrate; all the scale bars are 1 μm. (e) The transmittance of the transparent ITO/CuS NN composite films with different sheet resistance samples; the insets are photographs of the ITO/CuS NN composite films from A to C.

 This journal is © The Royal Society of Chemistry 2016

Published on 29 July 2016. Downloaded by Beijing Institute of Nanoenergy and Nanosystems CAS on 16/08/2016 02:10:30.

CuS NN, as shown in Fig. 1b. The diffraction peaks located at 27.6°, 29.3°, 31.8°, 48.1° and 59.2° as shown in Fig. 1b in the red line, corresponding to (101), (102), (103), (110) and (116) of a pure hexagonal CuS phase. Finally, ITO was sputtered onto the network to prepare ITO/CuS NN composite film. Fig. 1c shows the SEM images of the as-prepared ITO/CuS NN composite film with different scale bars. The morphology of the whole film is composed of the CuS NNs as the frameworks and ITO film fills in the open large space to enhance the uniformity of the metal nanotrough with small amounts of transmittance degradation. Each of the CuS nanosheets is ~2 μm in lengths and ~50 nm in width. Fig. 1d presents the energy-dispersive X-ray spectroscopy (EDS) images of the ITO/CuS NN composite films. Fig. 1d shows the distribution of Cu, S, In, Sn and O elements in the ITO/CuS NN composite film, indicating that ITO has been coated on the CuS nanosheet and distributed uniformly. The inserts in Fig. 1e display the transmittance of ITO/CuS NN composite films with different sheet resistances (from A to C). The lower transmittance of the ITO/CuS composite film corresponding to better conductance of the electrodes can be seen in Fig. 1e. Namely, there is a competition between the conductance and transmittance. The conductance is 11.6 Ω sq^{-1} (T = 46%) in the ITO/CuS NN composite film, and the value is comparable with that of CoS/ITO/PEN (T = 20%),[24] whereas the ITO/CuS NN composite film maintains good transparency in this work.

The mechanical durability is a benchmark characteristic for portable electronics. The CuS NN, ITO/CuS NN composite films and ITO/PET films were tested at different bending radii, as shown in Fig. 2a. Obviously, the CuS NN and the ITO/CuS NN composite films have superior mechanical endurance with negligible resistance increment, demonstrating excellent flexibility. However, the ITO/PET electrode has a sharp increment in resistance during bending tests due to its intrinsic brittleness. Fig. 2b illustrates the resistance evolution of ITO/CuS NN composite film after hundreds of repeats of bending with a bending radius of 5 mm. Both the CuS NN film and the ITO/CuS NN composite film exhibit robust stretchable properties with a slight increment during the bending cycle test, whereas the resistance of ITO is increased over several times. Fig. 2c shows that many cracks are formed after bending, indicating the poor mechanical stability of the ITO film. Fig. 2d shows the SEM images of the ITO/CuS NN composite film at different magnifications after bending. Since the CuS NN in the composite films can minimize the crack widths from the distribution of the cracks, rather than wide cracks, there are fewer cracks compared to neat ITO. To our knowledge, the overall mechanical performances reported here are the best among those in past research on CEs based on transparent conductive oxide materials.[9] The impressive flexibility of ITO/CuS NN composite film would greatly expand the application of traditional ITO electrodes in flexible DSSCs and wearable electronics.

The electrochemical catalytic properties of CEs are another benchmark for flexible DSSCs. Fig. 3a shows the CV curves of the ITO/CuS NN composite electrode with different ITO sputtering time; and among these electrodes, the 1 h ITO sputtering time composite electrode exhibits the best electrochemical catalytic properties. Fig. 3b shows the C–V curves of the ITO and the ITO/CuS NN composite electrode, respectively. Although ITO has been used in many optoelectronic devices as a transparent conductive electrode, its poor electrochemical catalytic properties hinder

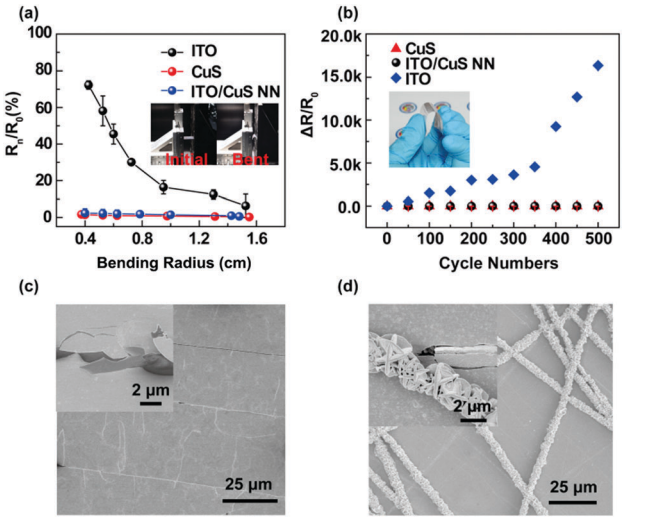

Fig. 2 (a) Plots show the bending effect on the normalized resistance of ITO film, CuS NN film and ITO/CuS NN composite film, respectively; the insets are the photographs of the bending test instruments from initial to bent; (b) the normalized resistance *versus* bending cycles with a bending radius of 5 mm; (c) the SEM images of ITO film after bending tests with different scale bars; (d) the SEM images of the ITO/CuS NN composite film after bending tests at different magnifications.

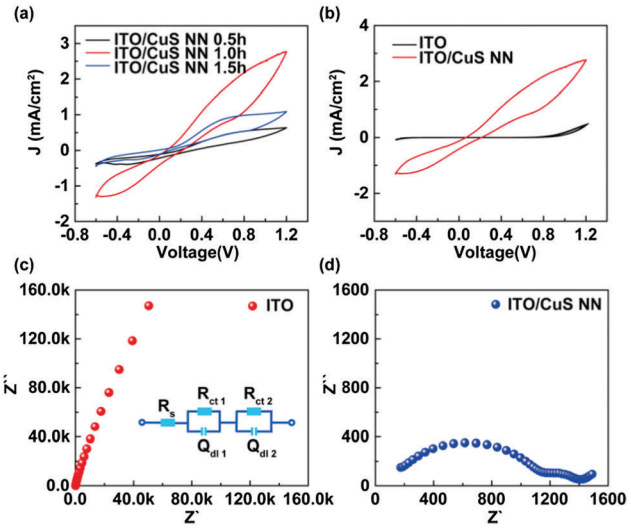

Fig. 3 (a) C–V curves of the CEs with the films of the ITO/CuS NN composite electrodes with different ITO sputtering time (0.5 h, 1 h, 1.5 h) and (b) C–V curves of the CEs with the films of the traditional ITO electrode and the ITO/CuS NN composite electrode obtained in the acetonitrile solution containing 10.0 mM LiI, 1.0 mM I_2, and 0.1 M $LiClO_4$, at a scan rate of 50 mV s^{-1}, respectively; (c) and (d) the EIS of the traditional ITO electrode and the ITO/CuS NN composite electrode in the same electrolyte, respectively.

Published on 29 July 2016. Downloaded by Beijing Institute of Nanoenergy and Nanosystems CAS on 16/08/2016 02:10:30.

Table 1 The photovoltaic parameters of the DSSCs based on the ITO electrode, CuS NN electrode and ITO/CuS NN composite electrode, respectively

Sample	J_{sc} [mA cm^{-2}]	V_{oc} [V]	PCE [%]	FF	R_{ct} [Ω cm^{-2}]
CuS/ITO	18.8	0.681	6	0.468	644.7
ITO	1.514	0.268	0.049	0.12	4583
CuS	18.10	0.66	6.38	0.534	21.95

its application in DSSCs. Superior electrochemical catalytic ability materials, *e.g.* Pt, CoS, graphene, carbon nanotubes and conducting polymers, have been coated on the ITO to enhance the catalytic properties. The superior electrochemical catalytic properties of the ITO/CuS NN composite electrode could just remedy the weaknesses of the traditional ITO electrode as a counter electrode without complex fabrication and high cost. The electrochemical impedance spectroscopy (EIS) was measured to investigate the electrocatalytic kinetics, and the resultant Nyquist plots are illustrated in Fig. 3c and d. The equivalent circuit model was used to fit Nyquist plots by Z-view software and the EIS parameters were obtained as shown in Table 1. The R_{ct} of the ITO/CuS NN composite electrode (644.7 Ω cm^{-2}), compared to the traditional ITO/PET electrode (4583 Ω cm^{-2}), exhibits a superior electrochemical catalytic ability as a counter electrode in the DSSCs. The ITO/CuS NN composite electrode has a large active surface area for the reaction of I^{3-}/I^{-} ions in electrolytes and will be a promising transparent conductive electrode for flexible DSSCs.

DSSCs, as the next generation of solar cells, are a kind of renewable, light-weight and low-cost power resource. The PCE is an essential standard to evaluate the performance of DSSCs. Fig. 4a illustrates a schematic image of the flexible DSSCs with the ITO/CuS NN composite films as CEs and the titanium dioxide nanotube arrays (TNARs) as photoanodes. Fig. 4b shows a photograph of the flexible DSSCs, which can be bent to a 2 cm radius. In Fig. 4c the PCE of the reported references on the traditional ITO electrode coated with different materials as counter electrodes is shown. According to Fig. 4c, the PCE of the ITO/CuS NN composite electrode was relatively high, whereas it was a little lower in FF, compared to the other materials from these references. The fabrication of the novel composite film is facile and much easier than the reported materials coated on ITO in preparation. Fig. 4d and e show the current density–voltage (J–V) characteristics of DSSCs with the ITO electrode[38] and the ITO/CuS NN composite electrode as CEs, respectively. The photovoltaic parameters are also listed in Table 1. The J_{sc}, V_{oc} and FF of the ITO/CuS NN based DSSC were 18.8 mA cm^{-2}, 0.681 V and 0.468, and the PCE of the ITO/CuS NN based DSSCs is 6% from Fig. 4e. However, the traditional ITO electrode has poor electrochemical catalytic properties and exhibits almost no photovoltaic efficiency as shown in Fig. 4d. The poor PCE of ITO cannot be used directly in the DSSCs as a counter electrode, whereas the new ITO/CuS NN has remedied the drawbacks of ITO, obtaining a relatively high PCE. In Fig. 4e, the ITO/CuS NN electrode has a slightly lower PCE compared to the CuS NN electrode, since ITO has coated the CuS NN and reduced the electrochemical catalytic properties slightly. Besides that, the current density of ITO/CuS NN based DSSCs is a little higher than the CuS NN electrode. Fig. 4f shows the normalized PCE (η_n/η_0) and the FF during the bending of a 2 cm bending radius, a slight decrease illustrated in the graphs after 200 cycles of folding and unfolding, which shows the good flexibility of the as-prepared DSSCs with ITO/CuS NN as the counter electrode. Above all, the ITO/CuS NN composite transparent conductive electrode has superior flexibility and good electrochemical catalytic properties, and can replace the traditional Pt-coated ITO electrode as CEs in the flexible DSSCs.

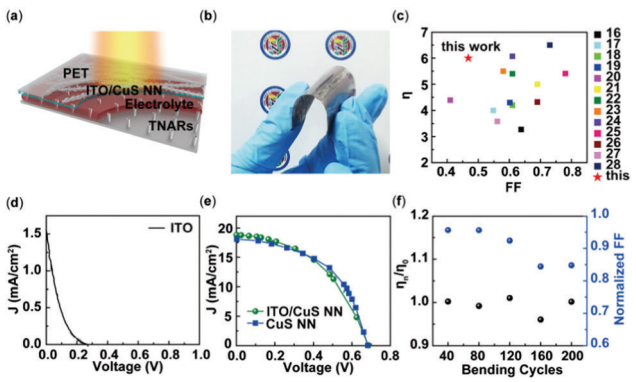

Fig. 4 (a) A corresponding schematic image and (b) a photograph of the as-prepared flexible DSSCs fabricated with the ITO/CuS NN composite electrodes as CEs and the TNARs/Ti foils as photoanodes; (c) previously reported counter electrodes of the flexible DSSCs from ref. 16–28, compared to this work in the relationship of power efficiency *versus* FF; (d) and (e) J–V curves of the DSSCs with the films of ITO electrode, CuS NN electrode and ITO/CuS NN composite electrode, respectively; light intensity is 100 mW cm^{-2} (AM 1.5); (f) the normalized PCE (η_n/η_0) of the ITO/CuS NN electrode in the flexible DSSCs as a function of bending cycles with a 2 cm bending radius.

Conclusions

We present the flexible transparent conductive ITO/CuS NN composite film with low sheet resistance and superior electrochemical catalytic properties. The composite films are employed as CEs in the fabrication of flexible DSSCs which achieve a PCE of 6%. After 200 bending cycles with a radius of 2 cm, the PCE shows negligible degradation. We believed that the flexible transparent conductive ITO/CuS NN composite electrode could be used in wearable and portable electronics and other collapsible gadgets in the future.

Acknowledgements

The authors are thankful for support from the ''Thousand Talents'' program of China for pioneering researchers and innovative teams and from the President Funding of the Chinese Academy of Sciences, National Natural Science Foundation of China (No. 51432005, 61405040, 61505010, 51502018 and U1404619), Beijing City Committee of science and technology (Z151100003315010).

 This journal is © The Royal Society of Chemistry 2016

Published on 29 July 2016. Downloaded by Beijing Institute of Nanoenergy and Nanosystems CAS on 16/08/2016 02:10:30.

References

1 B. Oregan and M. Gratzel, *Nature*, 1991, **353**, 737–740.
2 Y. J. Kim, M. H. Lee, H. J. Kim, G. Lim, Y. S. Choi, N. G. Park, K. Kim and W. I. Lee, *Adv. Mater.*, 2009, **21**, 3668–3673.
3 K.-M. Lee, L.-C. Lin, C.-Y. Chen, V. Suryanarayanan and C.-G. Wu, *Electrochim. Acta*, 2014, **135**, 578–584.
4 T. Miyasaka, *J. Phys. Chem. Lett.*, 2010, **2**, 262–269.
5 G. Hashmi, K. Miettunen, T. Peltola, J. Halme, I. Asghar, K. Aitola, M. Toivola and P. Lund, *Renewable Sustainable Energy Rev.*, 2011, **15**, 3717–3732.
6 V. Zardetto, F. Di Giacomo, D. Garcia-Alonso, W. Keuning, M. Creatore, C. Mazzuca, A. Reale, A. Di Carlo and T. M. Brown, *Adv. Energy Mater.*, 2013, **3**, 1292–1298.
7 K. Miettunen, J. Halme and P. Lund, *Wiley Interdiscip. Rev.: Energy Environ.*, 2013, **2**, 104–120.
8 I. Okada and S. Shiratori, *ACS Appl. Mater. Interfaces*, 2013, **5**, 4144–4149.
9 D. R. Cairns, R. P. Witte, D. K. Sparacin, S. M. Sachsman, D. C. Paine, G. P. Crawford and R. R. Newton, *Appl. Phys. Lett.*, 2000, **76**, 1425–1427.
10 Z. Chen, B. Cotterell and W. Wang, *Eng. Fract. Mech.*, 2002, **69**, 597–603.
11 L. Chen, W. Tan, J. Zhang, X. Zhou, X. Zhang and Y. Lin, *Electrochim. Acta*, 2010, **55**, 3721–3726.
12 T. N. Murakami and M. Grätzel, *Inorg. Chim. Acta*, 2008, **361**, 572–580.
13 X. Fang, T. Ma, M. Akiyama, G. Guan, S. Tsunematsu and E. Abe, *Thin Solid Films*, 2005, **472**, 242–245.
14 J. R. Brillet, D. Kuang, P. Chen, M. Takata, S. Uchida, H. Miura, K. Sumioka, S. M. Zakeeruddin and M. Grätzel, *ACS Nano*, 2008, **6**, 1113–1116.
15 D. Zhang, T. Yoshida, T. Oekermann, K. Furuta and H. Minoura, *Adv. Funct. Mater.*, 2006, **16**, 1228–1234.
16 P. Zhang, C. Wu, Y. Han, T. Jin, B. Chi, J. Pu, L. Jian and H. Hintzen, *J. Am. Ceram. Soc.*, 2012, **95**, 1372–1377.
17 M. G. Kang, N.-G. Park, K. S. Ryu, S. H. Chang and K.-J. Kim, *Sol. Energy Mater. Sol. Cells*, 2006, **90**, 574–581.
18 Y.-H. Wei, C.-S. Chen, C.-C. M. Ma, C.-H. Tsai and C.-K. Hsieh, *Thin Solid Films*, 2014, **570**, 277–281.
19 C.-K. Cheng and C.-K. Hsieh, *Thin Solid Films*, 2015, **584**, 52–60.
20 H. C. Weerasinghe, P. M. Sirimanne, G. V. Franks, G. P. Simon and Y. B. Cheng, *J. Photochem. Photobiol., A*, 2010, **213**, 30–36.
21 H. P. Jen, M. H. Lin, L. L. Li, H. P. Wu, W. K. Huang, P. J. Cheng and E. W. Diau, *ACS Appl. Mater. Interfaces*, 2013, **5**, 10098–10104.
22 W. Huang, X. L. Zhang, F. Huang, Z. Zhang, J. He and Y.-B. Cheng, *J. Nanopart. Res.*, 2012, **14**, 1–5.
23 L. L. Chen, J. Liu, J. B. Zhang, X. W. Zhou, X. L. Zhang and Y. Lin, *Chin. Chem. Lett.*, 2010, **21**, 1137–1140.
24 M. K. Wang, A. M. Anghel, B. Marsan, N. L. C. Ha, N. Pootrakulchote, S. M. Zakeeruddin and M. Gratzel, *J. Am. Chem. Soc.*, 2009, **131**, 15976–15977.
25 M. Ikegami, J. Suzuki, K. Teshima, M. Kawaraya and T. Miyasaka, *Sol. Energy Mater. Sol. Cells*, 2009, **93**, 836–839.
26 J. Y. Liao, B. X. Lei, H. Y. Chen, D. B. Kuang and C. Y. Su, *Energy Environ. Sci.*, 2012, **5**, 5750–5757.
27 S. Soltanian, R. Rahmanian, B. Gholamkhass, N. M. Kiasari, F. Ko and P. Servati, *Adv. Energy Mater.*, 2013, **3**, 1332–1337.
28 F. Xu and Y. Zhu, *Adv. Mater.*, 2012, **24**, 5117–5122.
29 R. Wang and H. Ruan, *J. Alloys Compd.*, 2016, **25**, 936–943.
30 W. He and C. Ye, *J. Mater. Sci. Technol.*, 2015, **31**, 581–588.
31 A. Elschner and W. Lövenich, *MRS Bull.*, 2011, **36**, 794–798.
32 S. Bae, H. Kim, Y. Lee, X. F. Xu, J. S. Park, Y. Zheng, J. Balakrishnan, T. Lei, H. R. Kim, Y. I. Song, Y. J. Kim, K. S. Kim, B. Ozyilmaz, J. H. Ahn, B. H. Hong and S. Iijima, *Nat. Nanotechnol.*, 2010, **5**, 574–578.
33 B. Friedel, T. J. K. Brenner, C. R. McNeill, U. Steiner and N. C. Greenham, *Org. Electron.*, 2011, **12**, 1736–1745.
34 M. Zhang, S. L. Fang, A. A. Zakhidov, S. B. Lee, A. E. Aliev, C. D. Williams, K. R. Atkinson and R. H. Baughman, *Science*, 2005, **309**, 1215–1219.
35 H. Wu, D. S. Kong, Z. C. Ruan, P. C. Hsu, S. Wang, Z. F. Yu, T. J. Carney, L. B. Hu, S. H. Fan and Y. Cui, *Nat. Nanotechnol.*, 2013, **8**, 421–425.
36 H. Wu, L. Hu, M. W. Rowell, D. Kong, J. J. Cha, J. R. McDonough, J. Zhu, Y. Yang, M. D. McGehee and Y. Cui, *Nano Lett.*, 2010, **10**, 4242–4248.
37 B. W. An, B. G. Hyun, S. Y. Kim, M. Kim, M. S. Lee, K. Lee, J. B. Koo, H. Y. Chu, B. S. Bae and J. U. Park, *Nano Lett.*, 2014, **14**, 6322–6328.
38 X. Zhang and W. Guo, *J. Mater. Chem. A*, 2016, **4**, 6569–6576.